Steel Containment Resistance Under General Dynamic Pressure

F. Fanous, L. Greimann
Iowa State Universtiy, Ames, IA USA

INTRODUCTION

Containment structures are important in minimizing the risk of radiological exposure of the public from severe accidents in a nuclear power plant. Failure of a containment is considered to take place when leakage occurs through shell plate. The capacity of a containment building to withstand loading beyond design basis has been subjected to extensive experimental and analytical research. Most, if not all, of this work focused on the effect of over pressurization on the containment performance (Clauss, 1985, Clauss, 1987, and Greimann, et. al. 1984). Besides uniform internal pressure, containment buildings may experience various types of loading that vary in time along both circumferential and meridional directions. Several methods ranging from a single degree-of-freedom-type approximation to a complete three-dimensional finite element shell model with material and geometric nonlinearities are available to analyze these variations. Considering the importance of the current problem, it seems reasonable to use a three-dimensional shell model. However, such an in-depth effort would not be practical for many containments on a case-by-case basis. For this reason, an intermediate approach that permits rapid analysis with reasonable accuracy would be useful. An axisymmetric approximation to the containment building that accounts for variation of the applied pressure as well as geometric imperfection is outlined herein. The nonsymmetric stress resultants obtained on the most stressed "worst" meridian from a dynamic analysis are assumed to be axisymmetric for the buckling analysis. To accomplish the axisymmetric analysis a computer program was written to interface modified versions of the (BOSOR4, 1975 and BOSOR5, 1975) finite difference codes.

NONSYMMETRIC DYNAMIC ANALYSIS

Pressures resulting from loss of coolant accident (LOCA) or safety relief valve blowdown could be nonuniformally distributed around the shell circumference, θ, and along the meridian, s, as illustrated in Fig. 1. If an axisymmetric shell analysis is used, the circumferential variation of the induced displacement and stress resultants are expressed by Fourier series as:

$$u(s,\theta,t) = \Sigma\, u_{an} \cos n\theta + \Sigma\, u_{bn} \sin n\theta \quad (1)$$

$$v(s,\theta,t) = -\Sigma\, v_{an} \sin n\theta + \Sigma\, v_{bn} \cos n\theta \quad (2)$$

$$w(s,\theta,t) = \Sigma\, w_{an} \cos n\theta + \Sigma\, w_{bn} \sin n\theta \quad (3)$$

$$N(s,\theta,t) = \Sigma\, N_{an} \cos n\theta + \Sigma\, N_{bn} \sin n\theta \quad (4)$$

in which u, v, and w are the shell meridional, circumferential, and radial displacements, respectively. The meridional, circumferential, and shear stress

resultants are expressed by Eq. (4). The Fourier coefficients u_{an}, u_{bn}, etc., where n = 1, 2, ----- number of harmonics, are functions of time and meridional coordinates. Dynamic equilibrium equations are written as:

$$[M]\{\ddot{u}(t)\} + [C]\{u(t)\} + [K]\{u(t)\} = \{F(t)\} \tag{5}$$

in which $\{u(t)\}$ are discrete nodal values of the Fourier coefficients. The mass, damping, and stiffness matrices are [M], [C], and [K], respectively. The nodal forces $\{F(t)\}$ are work equivalent to the applied pressure, p(s, ,t), which also can be represented in terms of Fourier series. The modal superposition approach (Bathe, 1976) was adopted in this work to solve Eq. 5. The solution of the modal equations is accomplish utilizing the Wilson-Θ method (Bathe, 1976). A value of 1.4 and an integration time step size less than one-tenth of the smallest natural period are used.

EQUIVALENT AXISYMMETRIC LOADS

The BOSOR5 finite difference computer code was used for the analysis of the axisymmetric model. To utilize this program, the stress resultants on the "worst" meridian was converted to equivalent axisymmetric pressure using the following governing differential equations for shell structures (Brush and Almroth, 1975):

$$\frac{\partial(rN_1)}{r\partial s} + \frac{\partial N_{12}}{r\partial\Theta} - \frac{N_2\cos\phi}{4} + \frac{1}{rr_1}\left[-\frac{\partial(rM_1)}{\partial s} + \frac{\partial M_{12}}{\partial\Theta} + M_2\cos\phi\right] = m\ddot{u} - p_u \tag{6}$$

$$-\frac{\partial\left(\partial(rM_1)\right)}{r\,\partial s^2} - \frac{\partial^2 M_2}{r^2\,\partial\Theta^2} + \frac{\partial(M_2\cos\phi)}{r\,\partial s} + \frac{2\partial^2(rM_{12})}{r^2\,\partial\Theta\partial s} - \frac{N_1}{r_1} - \frac{N_2}{r\sin\Theta} = m\ddot{w} - p_w \tag{7}$$

in which N_1, N_2 and N_{12} are the meriodional, circumferential and shear stress resultants, respectively and M_1, M_2 and M_{12} are the corresponding moment resultants. m is the mass per unit area, r, is radius of the meridian plan and the applied pressures are p_u and p_w. The acceleration terms on the right represent inertial pressures or, by D'alemberts' principle, the negative of equivalent static pressures.

NONLINEAR EXTRAPOLATION

In this work, an approximate nonlinear solution will be obtained by extrapolating the linear equivalent pressures (Greimann, at. al., 1986). This approach will be followed, however, on the basis that: (1) the extrapolation is not particularly extreme, that is, to a ductility of two at most; (2) the nonlinear behavior is, most likely, localized and controlled by the surrounding linear behavior; and (3) any unconservatism is probably offset by other conservatism, e.g., using the "worst" meridian approach. This approach is not inconsistent with the ASME Code that allows an elastic analysis for stresses beyond the yield strength for certain cases with limited plasticity (ASME Boiler and Pressure Vessel Code, 1980, Paragraph NE 3227.6).

FAILURE CRITERIA

Recently, investigators from Sandia National Laboratories (Clauss 1985) have predicted failure (leakage) as the point at which the calculated, equivalent membrane strain reaches a fraction of the material ultimate strain. This factor depends upon the degree of sophistication of the analysis model, the structural

detail available to the analyst, and variation in the material properties in the as-built containment. In this paper, failure of a containment vessel is taken to occur when the maximum membrane strain reaches twice the yield strain along the fundamental load path (plastic collapse) or when a bifurcation point is reached (buckling). In the second case, the membrane strains are assumed to go beyond twice the yield strain during the postbuckling stage. Membrane strains are used rather than surface (bending) strains, since the latter are often self-limiting, and, as such for ductile materials, have little effect on the collapse strength.

COMPUTER IMPLEMENTATION

Figure 2 illustrates a schematic of the containment analyzed herein. The stiffeners have rectangular cross sections of 36 in^2. An elastic, perfectly plastic material with a yield strength and modulus of elasticity of 50 ksi and 29,000 ksi, respectively, were used. To describe the pressure transients applied to the vessel, the wall is subdivided into five regions (Fig. 3). In real containments, the number of compartments is several times the number of regions used herein. Fig. 3(a) illustrates the pressure versus time transients in each region, and Fig. 3(b) shows the circumferential variation of the pressure at 0.3 seconds. A peak pressure of one psi was initially assumed and was increased by a factor m_p until failure of the containment building occurred.

BOSOR4 Analysis of Vibration Modes

The containment used in this example was modeled for BOSOR4 and BOSOR5 analysis using three shell segments with a total number of 159 mesh points. The finite difference element length was limited to rt/2, where r and t are the radius and wall thickness of the containment shell, respectively. No imperfection was included in the BOSOR4 model, since the vibration frequencies and modes are relatively insensitive to imperfection (BOSOR 4, 1975). A vibration mode analysis (INDIC=2) was used to solve for the natural frequencies, mode shapes, stress resultants, and the generalized mass and to evaluate the modal strains and stresses. The output from BOSOR4 was stored on files created during the execution for the upcoming dynamic analysis. The creation of these files has been added to the original BOSOR4 version.

Calculation of Equivalent Axisymmetric Pressures

The authors developed a routine to compute the equivalent pressures. The nonaxisymmetric pressure in Fig. 3 was expanded using eleven Fourier terms (n = 0, 1,---10) and a study was conducted using the most dominant terms in the Fourier expansion on the accuracy of the final results. The changes in the stress resultants over the shell structure were examined as the number of the meridional mode, m, was increased (see Fig. 4). Twenty meridional modes were used for n = 0 and forty were needed for n = 1, 2 and 3. The equivalent axisymmetric pressures were calculated every 0.03 seconds at zero, 45, 90, and 180 degrees meridional locations.

BOSOR5 Analysis of Containment Capacity

In BOSOR5 analysis the geometric imperfection was modeled as:

$$w_{imp} = w_o\left(1 - \cos\frac{2\,s}{L_o}\right) \tag{8}$$

where w_o is the radial imperfection amplitude (one-half the peak-to-trough amplitude of the imperfection), and L_o represents the wavelength of the axisymmetric imperfection. For stiffened shells, Seide, et. al., 1979 and

Bushnell, 1981 recommend different lengths according to the distance between ring stiffeners. Slight modifications to the BOSOR5 code were necessary in order to phase the imperfection with variable ring spacings. Also, the BOSOR5 code was modified to allow the user to read the point-by-point pressures for each time from the auxiliary file created during the execution of the BOSOR4 to BOSOR5 interface routine. The resistance of the containment is defined as the pressure, P_R, that has the same time and space distribution as the input pressure, p. The magnitude of the failure pressure is given by:

$$P_R\ (s,\theta,t) = m_p\ p(s,\theta,t) \tag{9}$$

where m_p is a pressure multiplier which is found by the following procedure: (1) select a meridian at θ; (2) for a selected value of m_p, input the time history of the equivalent axisymmetric pressures into the modified BOSOR5 program in order to evaluate the shell strains and check stability at all times; (3) increase m_p until strains reach twice the yield or bifurcation buckling occurs; (4) examine all meridians, i.e., at θ = 0, 45, 90 and 180 until the "worst" is found.

Figure 5 illustrates the relationship between this maximum membrane strain and the pressure multiplier at θ = 0 ("worst" meridian). From the figure, the maximum membrane strain reached twice the yield value with a pressure multiplier of 110. This represents a peak dynamic pressure of 110 psi at 0.3 seconds in region 2 (see Fig. 3).

The final step in the containment analysis is to investigate the stability using the BOSOR5 code. For circumferential wave numbers ranging from 0 to 50 and a pressure multiplier of 110, a bifurcation point did not occur. Therefore, the failure pressure of the containment example, is controlled by plastic collapse.

SUMMARY AND CONCLUSIONS

A simple methodology that permits rapid and reasonably accurate analysis of the capacity of steel containment buildings under spatially varying dynamic loadings was developed. An axisymmetric model was used and the circumferential variation of the pressure was presented by Fourier series. Shell vibration and buckling analyses were performed utilizing modified versions of BOSOR4 and BOSOR5 finite difference codes, respectively. Consistent with the use of an axisymmetric model, an axisymmetric "worst meridian" prebuckled shape was used to investigate buckling. This methodology was implemented into a computer program that interfaced BOSOR4 and BOSOR5 codes to analyze a simplified containment building. Efforts required to model a containment and computer time are minimal compared to a three-dimensional finite element analysis.

REFERENCES

ASME Boiler and Pressure Vessel Code. (1980). Sec. III. Class MC Components. Subsection NE. Paragraphs 3331-3335.

Bathe, K. J. and Wilson, E. D. (1976). Numerical Methods in Finite Element Analysis, Prentice-Hall, Englewood Cliffs, New Jersey.

Brush, D.O. and Almroth, B.O. (1975). Buckling of Bars, Plate, and Shells. McGraw Hill. New York.

Bushnell, D. (1981). Plastic Buckling of Various Shells. Proc. of the ASME/ASCE Mechanics Conference. Boulder, CO.

Bushnell, D. (1975). BOSOR4 Program for Stress, Buckling and Vibration Complex Shells of Revolution. Structural Mechanics Laboratory. Lockheed Missiles and Space Co., Inc., Palo Alto, CA.

Bushnell, D. (1975). BOSOR5 Program for Buckling of Elastic-Plastic Complex Shells of Revolution Including Large Deflections and Creep. Structural Mechanics Laboratory. Lockheed Missiles and Space Co., Inc., Palo Alto, CA.

Clauss, D. B. (1985). Comparison of Analytical Prediction and Experimental Results for a 1:8 Steel Containment Model Pressurized to Failure. NUREG/CR-4209, SAND85-0679. Sandia National Laboratories, Albuquerque, NM.

Clauss, D. B. (1987). Round Robin Pretest Analysis of a 1:6 Scale Reinforced Concrete Containment Model Subjected to Internal Pressurization. NUREG/CR-4913, SAND87-0891. Sandia National Laboratories, Albuquerque, NM.

Greimann, L. F., Fanous, F., and Bluhm, D.(1984). Containment Analysis Techniques. A State-of-the-Art Summary. NUREG/CR3653.SAND83-7463. Sandia National Laboratories, Albuquerque, NM.

Greimann, L. F., Fanous, F., and Bluhm, D. (1986). Steel Containment Resistance Under General Dynamic Pressure. NUREG/CR4223, U.S. Nuclear Regulatory Commission.

Seide, P., Weingarten, V., and Masri, S. (1979). Buckling Criteria and Application of Criteria to Design of Steel Containment Shells. Report to NRC. NUREG/CR-0793, May 1979.

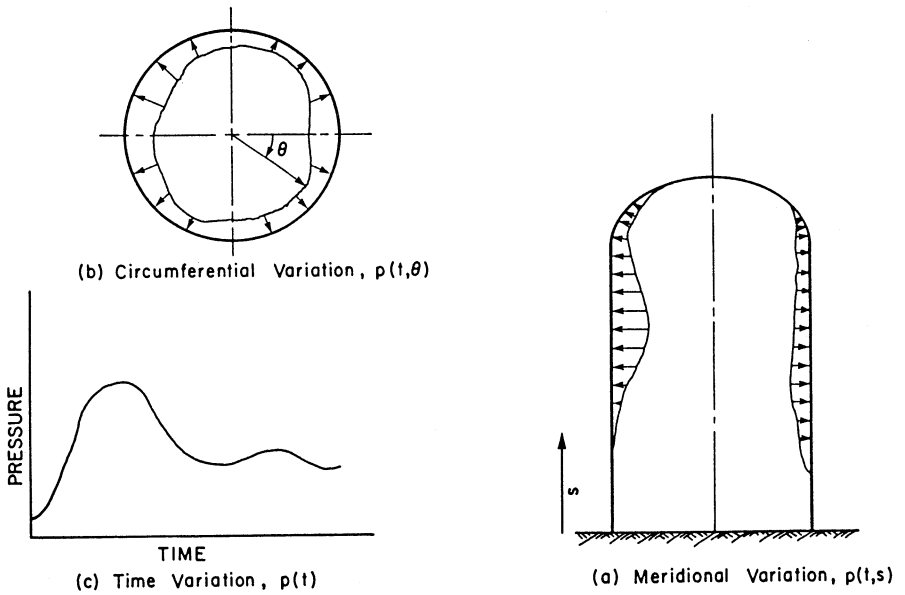

Figure 1. Pressure variation within a containment vessel.

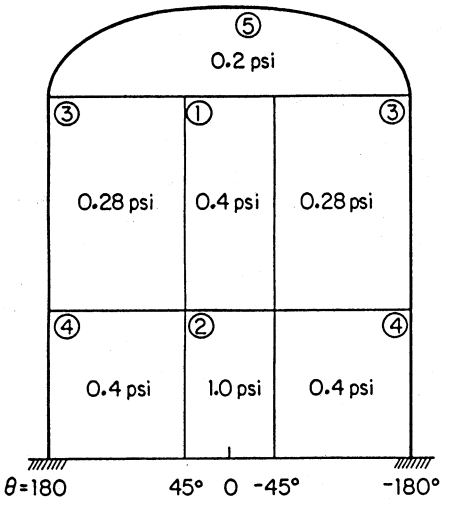

(b) Pressure Circumferential Distribution in the Five Regions at Time = 0.3 Sec.

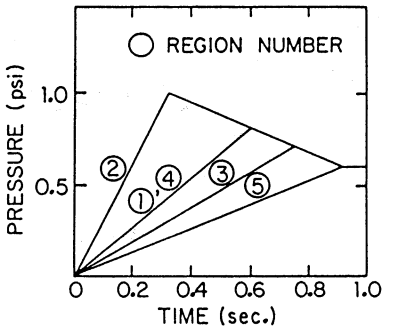

(a) Pressure Time Relationship for the Five Regions

Figure 3. Pressure transients used in the containment vessel analysis in Sec. 7.

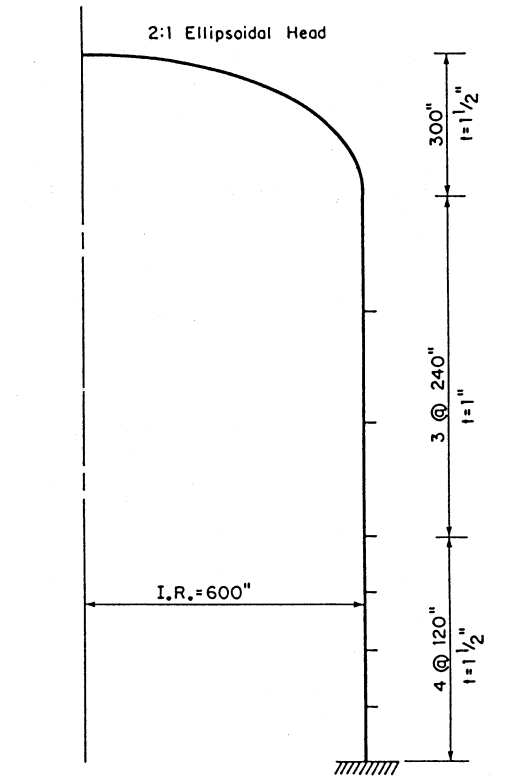

Figure 2. Containment vessel geometry.

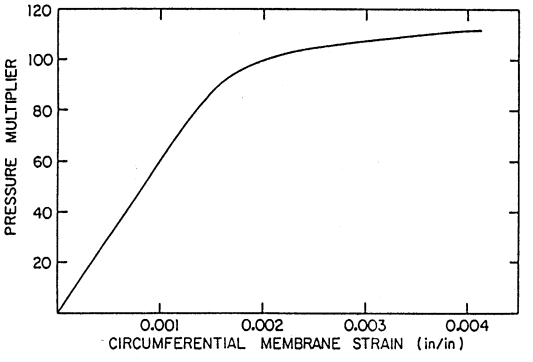

Figure 5. Circumferential membrane strain at Θ = zero and between lower rings for the containment shown in Fig. 3.

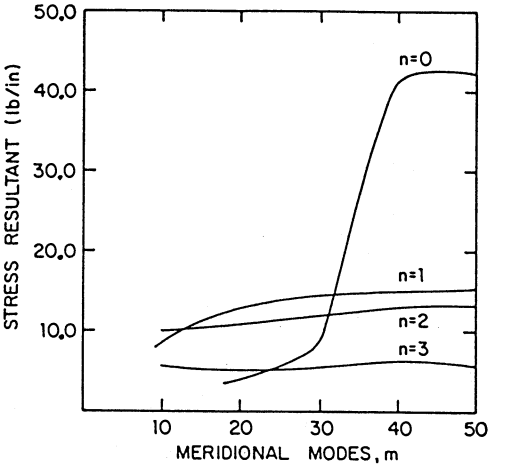

Figure 4. Effects of the meridional modes on the maximum circumferential stress resultants in Region Two (0.3 sec.).